Mathematica package for analysis and control of chaos in nonlinear systems

José Manuel Gutiérrez[a)] and Andrés Iglesias[b)]
Department of Applied Mathematics, University of Cantabria, Santander 39005, Spain

(Received 27 April 1997; accepted 27 July 1998)

In this article a symbolic Mathematica package for analysis and control of chaos in discrete and continuous nonlinear systems is presented. We start by presenting the main properties of chaos and describing some commands with which to obtain qualitative and quantitative measures of chaos, such as the bifurcation diagram and the Lyapunov exponents, respectively. Then we analyze the problem of chaos control and suppression, illustrating the different methodologies proposed in the literature by means of two representative algorithms (linear feedback control and suppression by perturbing the system variables). A novel analytical treatment of these algorithms using the symbolic capabilities of Mathematica is also presented. Well known one- and two-dimensional maps (the logistic and Hénon maps) and flows (the Duffing and Rössler systems) are used throughout the article to illustrate the concepts and algorithms. © *1998 American Institute of Physics.* [S0894-1866(98)01806-9]

INTRODUCTION

In recent years, increasing research activity in the field of nonlinear systems has shown that simple dynamical models can produce complex, seemingly random-looking behavior, including the appearance of *deterministic chaos*. One of the main features of deterministic chaos is its sensitive dependence to the initial conditions. This means that the separation between two nearby orbits of the system grows exponentially in time and, therefore, a long-term prediction of the system is possible only in probabilistic terms, although the system dynamics is described by deterministic equations (deterministic chaos). The inability to predict the behavior of dynamical systems in the presence of chaos makes this situation undesirable in many practical situations (electronic circuits, chemical reactions, etc.), where one is more interested in obtaining regular behavior. However, the possibility of controlling chaos offers a way to avoid this problem. As we shall see, the different controlling algorithms proposed in the literature take advantage of the deterministic nature of chaotic systems that defines some regularity in their inner structure.

In this article we introduce a Mathematica package that includes several tools both for analyzing discrete and continuous systems and for controlling the chaotic behavior appearing in these systems (this package is available at the World Wide Web site http://ccaix3.unican.es/~gutierjm/software.html). First, we introduce the basic properties of nonlinear systems using the commands of the package that apply in this situation. For instance, these commands allow us to obtain periodic points and their stability regions of nonlinear systems as well as some qualitative and quantitative measures of chaos, such as the bifurcation diagram and the Lyapunov exponents, respectively. Next, we analyze the problems of chaos control and suppression by presenting their main ideas and illustrating the different approaches by means of two representative algorithms: the linear-feedback-control method and algorithm suppression by perturbing the system variables. We also present a novel analytical treatment of these algorithms using the symbolic capabilities of Mathematica.

To illustrate the concepts and algorithms presented in the article, we use well-known examples of discrete maps (the logistic and Hénon maps) and continuous flows (the Duffing oscillator and the Rössler system). We also give the code of some of the commands to illustrate the programming style and the symbolic and functional capabilities of Mathematica. However, for a full understanding of these programs some knowledge on Mathematica is required (see Ref. 1).

I. SYMBOLIC ANALYSIS OF NONLINEAR SYSTEMS

One of the most popular and simple examples of the nonlinear dynamical system is the *logistic map*, which is given by the quadratic map $x_{n+1}=f(r,x_n)=rx_n(1-x_n)$, defined on the unit interval (0,1), for values of the parameter $r \in [0,4]$, and on the interval $[-(1/2),(3/2)]$ for $r \in [-2,0]$.

```
Logistic[r_]:=Function[x, r x (1−x)];
```

This map was originally used by ecologists to model population growth.[2] Given an initial population x_0, the next year's population is given by $x_1=f(r,x_0)$, where the parameter r is a growth rate. Repeating this iterative process, $x_2=f(r,x_1)$, and so on, the sequence of populations corresponding to successive years is obtained. This sequence is called the *orbit* of the point x_0. The powerful Mathematica functional-programming techniques help us to

[a)] E-mail: gutierjm@ccaix3.unican.es; http://ccaix3.unican.es/~gutierjm
[b)] E-mail: iglesias@ccaix3.unican.es; http://ccaix3.unican.es/~iglesias

© 1998 AMERICAN INSTITUTE OF PHYSICS 0894-1866/98/12(6)/608/12/$15.00

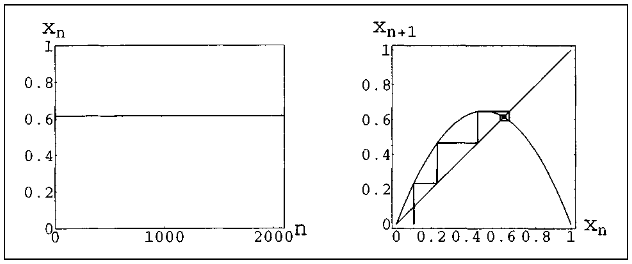

Figure 1. Time series (left) and first return map (right) of the fixed point logistic map with r =2.6 and x_0 =0.1

implement several algorithms for computing orbits in an intuitive and efficient form. For example, the command Orbit[map, x0, n] uses the NestList functional command to compute the n-point orbits of the map associated with the initial condition $x0$. On the other hand, the command IterativeProcess[map, x0, {min,max}] illustrates the iterative process $(x_n,x_{n+1})\to(x_{n+1},x_{n+1})\to(x_{n+1},x_{n+2})$ in the delay reconstruction phase space (x_n,x_{n+1}).

```
Orbit[map_,x0_,n_]:=NestList[map, x0, n];
IterativeProcess[map_,x0_,{min_,max_}]:=
Module[{fr,orb},
  orb=Orbit[map,x0,50];
  fr=MapThread[Line[{{#1,#1},{#1,#2},{#2,#2}}]&,
      {Drop[orb,−1],Drop[orb,1]}];
  Show[Plot[{map[x],x},{x,min,max}], Graphics[{fr}]] ]
```

With the help of these commands we can analyze the different system behaviors depending on the values of the growth parameter. For certain values of this parameter, the population settles to a fixed size over the years. This is called a *fixed point* of the system (see Fig. 1).

```
Show[GraphicsArray[
  {ListPlot[Orbit[Logistic[2.6],0.1,100]],
  IterativeProcess[Logistic[2.6],0.1,{0,1}]}]]
```

When the parameter value is increased, the system jumps back and forth between two different points. This is called a *period-2 orbit* (see Fig. 2).

```
Show[GraphicsArray[
  {ListPlot[Orbit[Logistic[3.2],0.1,100]],
  IterativeProcess[Logistic[3.2],0.1,{0,1}]}]]
```

In addition, the system may also evolve under an infinite number of points in a random-looking form (see Fig. 3). This behavior is known as deterministic chaos, since seemingly stochastic (chaotic) behavior is obtained from the dynamics of a deterministic system.

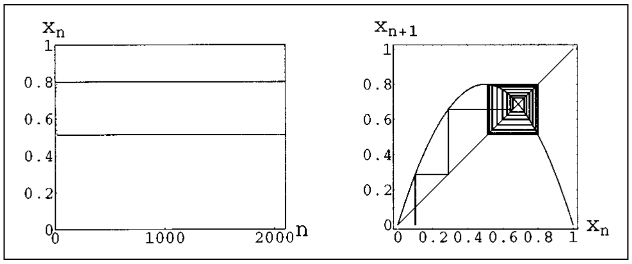

Figure 2. Time series (left) and first return map (right) of the period-2 logistic map with r =3.2 and x_0 =0.1

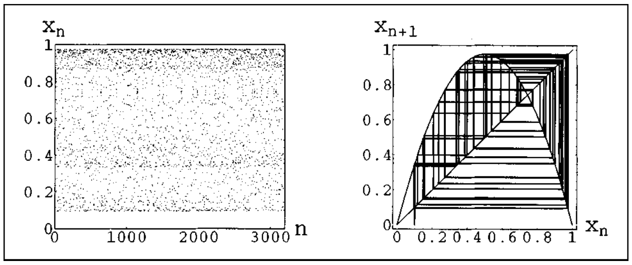

Figure 3. Time series (left) and first return map (right) of the chaotic logistic map given by r =3.9 and x_0 =0.1

```
Show[GraphicsArray[
  {ListPlot[Orbit[Logistic[3.9],0.1,100]],
  IterativeProcess[Logistic[3.9],0.1,{0,1}]}]]
```

The different behaviors of the system for different values of the parameter can be qualitatively analyzed by using a *bifurcation diagram*, which is created by plotting the asymptotic orbits of the maps (y axis) generated for different values of the parameter (x axis). The command Bifurcation[map, {p,pi,pf,np}, n] plots the bifurcation diagram of the *map* consisting of n-point orbits (after discarding an initial transient) for *np* equally spaced parameters in the region $p=pi$ to pf.

```
Bifurcation[map_, {p_, pi_, pf_, np_}, n_]:=
Module[{pp},ListPlot[Flatten
  [Table[({pp,#})& /@ Drop[Orbit[map /. p→pp][0.5,n
  +50],50], {pp,pi,pf,(pf−pi)/np}],1],
  Axes→False,Frame→True,
  PlotStyle→{PointSize[0.003]}]]
```

As an example, Fig. 4 shows the complete bifurcation diagram of the logistic map, considering all the possible values of the parameter in the range (−2,4). Note that the logistic map is usually defined for the parameter range (0,4), where the population of the system is normalized (defined by the unit interval) and the parameter takes on positive values. A detail of this region is shown in the inset of Fig. 4.

```
Show[Graphics[{Rectangle[{0,0},{1,1},
  Bifurcation[Logistic[r],{r,−2,4,250},0.5,200,]],
  Rectangle[{0.3,0.5},{0.7,1},
  Bifurcation[Logistic[r],{r,0,4,100}, 0.5,200]]}]]
```

The dynamics observed in Figs. 1–3 can now be better understood with the help of the bifurcation diagram. When the value of the parameter r is increased from zero, the system dynamics follow a sequence of period-1, -2, -4,...

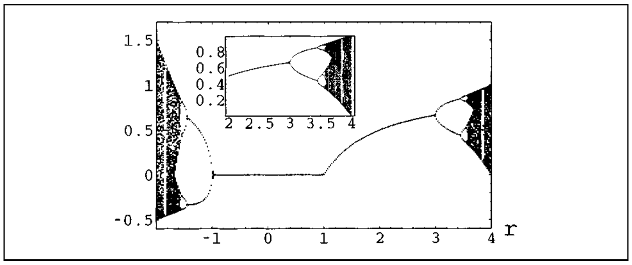

Figure 4. Bifurcation diagram for the logistic map. The inset was created by zooming into the region r =2–4.

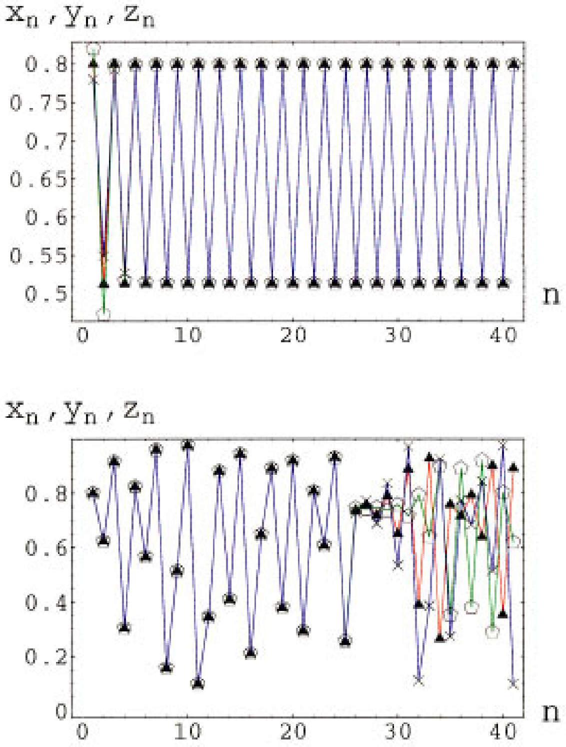

Figure 5. Three different orbits, x_n, y_n, and z_n (in different colors), corresponding to a periodic logistic map with initial conditions 0.8, and 0.8±0.02 (upper panel) and to a chaotic map with initial conditions 0.8 and 0.8 ± 10^{-8} (lower panel).

orbits called *period-doubling bifurcation route to chaos*. This sequence has universal properties for a large class of maps (for further details we refer the interested reader to Ref. 12). When the parameter r is chosen beyond the critical accumulation parameter $r_c=3.569...$, the system becomes unpredictable and exhibits deterministic chaos. Therefore, in this map deterministic chaos appears as a consequence of the accumulation of an infinite number of unstable periodic orbits resulting of the period-doubling bifurcation process. This is another interesting property of chaos known as *orbit complexity* (see Ref. 4). Orbit complexity means that chaotic systems contain an infinite number of unstable periodic orbits (UPOs), which coexist with the strange attractor and play an important role in the system dynamics.[5] This fact will be used later to control chaotic behavior by stabilizing some of these unstable orbits.

As we have already mentioned, the difference between regular and chaotic behaviors can be established in terms of their dependence on the initial conditions (or perturbations of the orbit). As shown in Fig. 5, periodic orbits are insensitive to large perturbations of the initial conditions, whereas chaotic orbits are very sensitive to tiny perturbations.

```
MultipleListPlot[Orbit[Logistic[3.2],#,40]& /@
      {0.8, 0.8+0.02, 0.8−0.02}]
  MultipleListPlot[Orbit[Logistic[3.9],#,40]& /@
      {0.8, 0.8+10^(−8), 0.8−10^(−8)}]
```

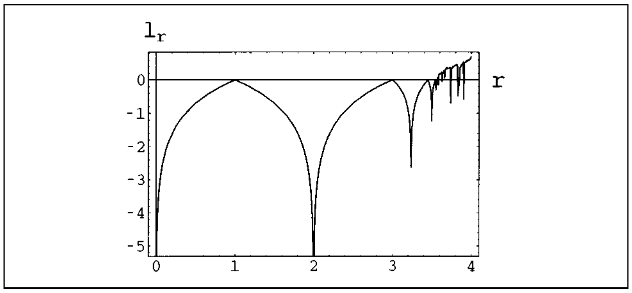

Figure 6. Lyapunov exponent l_r of the logistic map.

A quantitative measure of the sensitive dependence to initial conditions is given by the Lyapunov exponents, which measure the exponential separation of nearby orbits. In simple terms, a positive Lyapunov exponent can be considered to be an indicator of chaos, whereas negative exponents are associated with regular behavior (periodic orbits). The command LyapunovExp[map,x0,n] calculates the Lyapunov exponent of the one-dimensional (1D) map working with an n-point orbit starting at $x0$. In this case, this exponent can be easily obtained by averaging the logarithms of the map derivatives along the orbit.[3]

```
LyapunovExp[map_,x0_,n_]:=Plus @@ (
  Function[x,Evaluate[Log[Abs[D[map[x],x]]]]] /@
  Drop[Orbit[map, x0, n+500],500])/n
```

As an example, Fig. 6 shows the Lyapunov spectrum of the logistic map in the parameter range (0,4). If we compare Fig. 6 with the bifurcation diagram shown in the inset of Fig. 4, we can see how periodic regimes are associated with negative Lyapunov exponents, whereas chaotic ones have positive exponents.

```
Plot[Lyapunov[Logistic[r],0.5,500],{r,0,4}]
```

The rich structure of the bifurcation diagram and, hence, of the system dynamics is a consequence of the stable or unstable character of the periodic points for different values of the parameter. A fixed point x_f is *stable* if and only if it attracts nearby orbits, i.e.,

$$|[\partial_x f(r,x)]_{x_f}|<1,$$

and unstable otherwise.
The command PeriodicPoints[map, x, n] obtains the period-n fixed points of the map and the command Stability[map, x, r, fp, n] gives the regions for the parameter r where the period-n points fp are stable.

```
FixedPoints[map_,x_,n_]:=  Simplify[Solve[Nest[map,x,n]
==x,x]];
PeriodicPoints[map_,x_,n_]:=
  x/. Complement[FixedPoints[map,x,n],FixedPoints[map,x,
  n-1]];
Stability[map_,x_,r_,fp_,n_]:=
Module[{equ,s1,s2},
  equ=D[Nest[map,x,n],x] /. x→fp;
  {s1,s2}=Solve[equ==#, r]& /@ {−1,1};
  If[s1!={} && s2!={}, Sort /@
    MapThread[List, {Flatten[r/. s1],Flatten[r/. s2]}],{}] ]
```

These commands help us to analyze the bifurcation structure of the logistic map in an analytical form. For example, the period-one points of the logistic map are

```
p1=PeriodicPoints[Logistic[r],x,1]
```

$$\left\{0,\frac{r-1}{r}\right\}$$

which remain stable within the parameter regions $(-1,1)$ and $(1,3)$, respectively, as obtained below.

```
Stability[Logistic[r],r,#,x,1]& /@ p1
```

$$\{\{\{-1,1\}\},\{\{1,3\}\}\}$$

Therefore, if $-1<r<1$, the fixed point $(r-1)/r$ is unstable, whereas zero is stable. This implies that every trajectory of the system will asymptotically fall to zero. However, as r increases, the system presents a *tangent bifurcation* where the fixed point 0 loses its stability and the fixed point $(r-1)/r$ becomes stable [see interval (1,3) in Fig. 4]. For larger values of the parameter, the fixed point $(r-1)/r$ becomes unstable and splits up into two different period-2 points:

```
p2=PeriodicPoints[Logistic[r],x,2]
```

$$\left\{\frac{1+r-\sqrt{-3-2r+r^2}}{2r},\frac{1+r+\sqrt{-3-2r+r^2}}{2r}\right\}$$

whose stability intervals are

```
Stability[Logistic[r],r,#,x,2]& /@ p2
```

$$\{\{\{-1,1-\sqrt{6}\},\{3,1+\sqrt{6}\}\},\{\{-1,1-\sqrt{6}\},\{3,1+\sqrt{6}\}\}\}$$

In this case we have two stability regions for each of the fixed points. Then, four period-4 points become stable, and so on. Note that the calculation of periodic points with larger periodicities involves polynomials of degrees larger than five and, therefore, in general, they can only be obtained numerically. In this case, the command NFixedPoints[map, x, n] gives all the periodic points of the map up to period n. For example, to illustrate the orbit complexity phenomenon characteristic of chaotic systems, we can use this command to obtain all the unstable periodic points up to a given period (e.g., $n=8$) coexisting with the chaotic attractor of the logistic map:

```
NFixedPoints[Logistic[3.9],x,8]

     {0.,0.00570386,0.00717971,0.0636502,0.0656863,0.0691803,0.0750764,
     0.0917974,0.0919389,0.0974435,0.100562,0.104305,0.111837,0.114523,
     0.121947,0.124823,0.132653,0.156816,0.180986,0.213536,0.237367,
     0.289332,0.301209,0.358974,0.358974,0.385122,0.388375,0.413084,
     0.43037,0.448718,0.465846,0.467459,0.476801,0.578097,0.619508,
     0.697677,0.71665,0.74359,0.74359,0.74359,0.74359,0.75911,0.801914,
     0.803777,0.827517,0.848259,0.897436,0.897436,0.9193,0.951213,0.964744}
```

This phenomenon of creation and destruction of fixed points as a transition to chaos is also present in higher-dimensional discrete and continuous systems such as, for example, the Hénon map:[6]

$$(x_{n+1},y_{n+1})=f(r,x_n,y_n)=(1-rx_n^2+y_n,\tfrac{1}{3}x_n).$$

```
Henon[r_] :=
     Function[x,{1-r x[[1]]^2+x[[2]], 1/3 x[[1]]}]
```

Depending on the values of the parameter r, this system evolves among different behaviors associated with chaotic dynamics (transient chaos, interior crisis, etc.).[7] For example, the system exhibits deterministic chaos for $r=1.282$. The bifurcation diagram associated with one of the variables, say x, can be obtained as in the previous case (see Fig. 7):

```
Bifurcation[Henon[r],{r,0,1.3,250},{0.5,0.5},150]
```

In this case, we can also obtain the periodic points, forming the period-doubling route to chaos, and study their stability. For example, the period 1 and 2 points for the Hénon map can be obtained by

```
p1=PeriodicPoints[Henon[r],{x,y},1]
```

$$\left\{\left\{-\frac{1+\sqrt{1+9r}}{3r},-\frac{1+\sqrt{1+9r}}{9r}\right\},\right.$$
$$\left.\times\left\{\frac{-2+\sqrt{4+36r}}{6r},\frac{-2+\sqrt{4+36r}}{18r}\right\}\right\}$$

```
p2=PeriodicPoints[Henon[r],{x,y},2]
```

$$\left\{\left\{\frac{1+\sqrt{-3+9r}}{3r},-\frac{-1+\sqrt{-3+9r}}{9r}\right\},\right.$$
$$\left.\times\left\{-\frac{-1+\sqrt{-3+9r}}{3r},\frac{1+\sqrt{-3+9r}}{9r}\right\}\right\}$$

In this case, the stability of the fixed points depends on the eigenvalues of the corresponding Jacobian matrix:

```
ev=Eigenvalues[D[Henon[r][{x,y}],#]& /@{x,y}]
```

$$\{\tfrac{1}{6}(-6rx-\sqrt{12+36r^2x^2}),\ \tfrac{1}{6}(-6rx+\sqrt{12+36r^2x^2})\}$$

The next command shows that all these points are unstable, since they have associated a positive eigenvalue that defines an unstable manifold. Fixed points with both positive and negative eigenvalues are called *saddle nodes* and define stable and unstable manifolds. These points play a key role in the context of chaos control.[8]

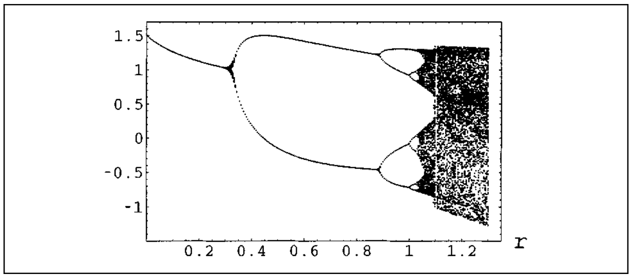

Figure 7. Bifurcation diagram of the Hénon map.

```
(ev //. {x→#[[1]],r→1.282})& /@ Union[p1,p2]
```

$$\{\{-0.2218,1.503\},\{-2.736,0.1218\},\{-0.1064,3.134\},$$
$$\{-1.872,0.1781\}\}$$

Figure 8 shows the strange attractor (chaotic orbit) of the Hénon map for $r=1.282$ and $(x_0,y_0)=(0.5,0.5)$. Figure 8 also shows the periodic points obtained above.

```
MultipleListPlot[Orbit[Henon[1.282],{0.5,0.2},2000],
  p1/.r→1.282,p2/.r→1.282]
```

Deterministic chaos is also present in continuous nonlinear systems given by flows, i.e., systems of differential equations. One of the most popular continuous nonlinear systems is the Duffing oscillator, which includes damping and periodic external forcing terms and is given by the following second-order differential equation:[9]

$$x''+ax'+x^3-x=f\ \cos(\omega t),$$

or, equivalently, by the system of three first-order differential equations

$$\begin{cases} x'=v \\ v'=-av-x^3+x+f\ \cos(z),, \\ z'=\omega \end{cases}$$

where $v=x'$, $z=\omega t$, a is the constant damping, and f and ω are the strength and the frequency of the external forcing, respectively. By fixing the values of constant damping and external frequency, the oscillator exhibits a great variety of behaviors as a function of the parameter f. In this example, we take $a=0.5$ and $\omega=1$.

```
Duffing[f_,w_]:={v, −1/2*v−x^3+x+f* Cos[z], w};
```

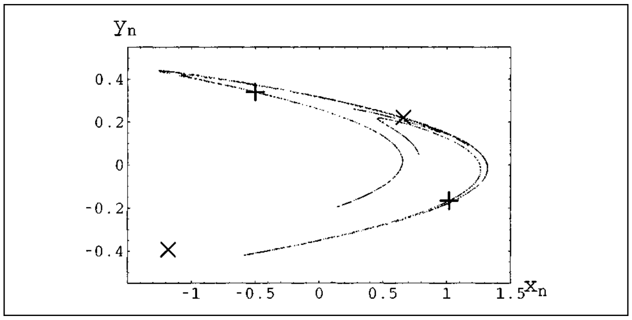

Figure 8. Chaotic attractor of the Hénon map with two period-one and two period-two points labeled as × and +, respectively.

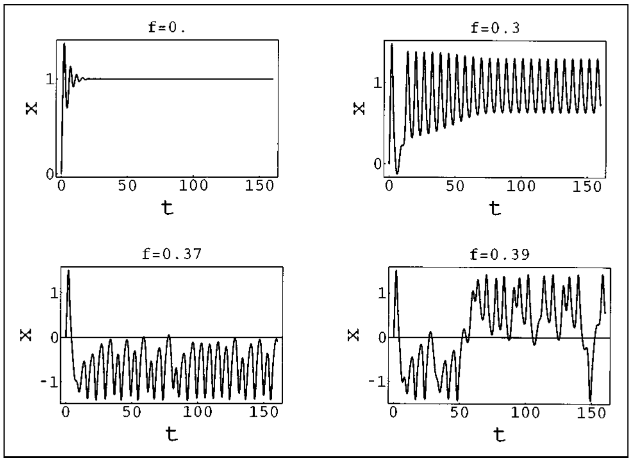

Figure 9. Dynamics of the Duffing oscillator for different values of the external forcing f.

The fixed points of a flow can be obtained using the command FixedPointsFlow[flow,vars]. In the case of the nonlinear oscillator, in the absence of external forcing ($f=0$), the system has two stable fixed points at $x=-1$ and $x=1$ (the positive one is shown in Fig. 9 labeled $f=0$).

```
fp=FixedPointsFlow[Duffing[0,w], {x,v,z}]
```

$$\{\{v\to 0,x\to -1\},\{v\to 0,x\to 0\},\{v\to 0,x\to 1\}\}$$

The stability of these fixed points is given by the eigenvalues of the corresponding Jacobian matrix:

```
ev=Eigenvalues[D[Duffing[0,w],#]& /@{x,v,z}]
```

$$\{0,\ \tfrac{1}{4}(-1-\sqrt{17-48x^2}),\ \tfrac{1}{4}(-1+\sqrt{17-48x^2})\}$$

The eigenvalues corresponding to each of the above fixed points are

```
Re[ev /.fp]
```

$$\{\{0,-\tfrac{1}{4},-\tfrac{1}{4}\},\{0,\ \tfrac{1}{4}(-1-\sqrt{17}),\ \tfrac{1}{4}(-1+\sqrt{17})\},$$
$$\times\{0,-\tfrac{1}{4},-\tfrac{1}{4}\}$$

Therefore, $x=-1$ and $x=1$ are two stable fixed points (negative real parts of the eigenvalues) and $x=0$ is an unstable fixed point. When some forcing is applied to the system, all the points become unstable and the system oscillates around one of the fixed points with frequency equal to the external frequency ω (Fig. 9, $f=0.3$). For values of the parameter $f>0.321$ the system goes through a period-doubling route to chaos. This period-doubling process has an accumulation point at $f_c=0.3586$. Therefore, larger values of the parameter lead to a chaotic system. For $f_c<f<0.386$, the chaotic orbits of the system remain trapped at one of the wells oscillating around a fixed point. For example, Fig. 9 ($f=0.37$) shows a chaotic orbit oscillating around the unstable fixed point $x=-1$. When increasing the value of the parameter, the strange attractor encompasses both wells (Fig. 9, $f=0.39$).

The command OrbitFlow[flow, x, x0, {t0,t1,dt}] implements a fourth-order Runge-Kutta method for systems of first-order differential equations. This command is used in the next example to calculate and plot several orbits, illustrating different behaviors of the Duffing oscillator.

```
Show[GraphicsArray[Show[
  OrbitFlow[Duffing[#,1],{x,v,z},{0.,1.,0.},{0,160,0.05},
  Show→Plot]& /@{0.,0.3,0.37,0.39}] ]]
```

II. SELECTING UNSTABLE PERIODIC ORBITS

As we have indicated in Sec. I, the infinite number of unstable periodic orbits (UPOs) embedded in the attractor plays an important role in the behavior of chaotic systems. However, in many practical situations one does not have access to system equations and must deal directly with experimental data in the form of a time series.[10] Here in Sec. II we give some commands for computing some of these orbits from a time series of the system (these commands will be used later for controlling chaos).

A simple algorithm for obtaining a UPO searches for closed ''orbits'' within the time series. Suppose we choose an arbitrary point of the time series and wait until the orbit comes back again to a small neighborhood of the selected point (the return neighborhood). Then, we may conclude that the orbit obtained shadows an unstable periodic orbit of the system.[10] The command UPO[timeseries, ϵ, maxper] obtains all the UPOs within the time series up to period *maxper* considering ϵ-radius balls as return neighborhoods.

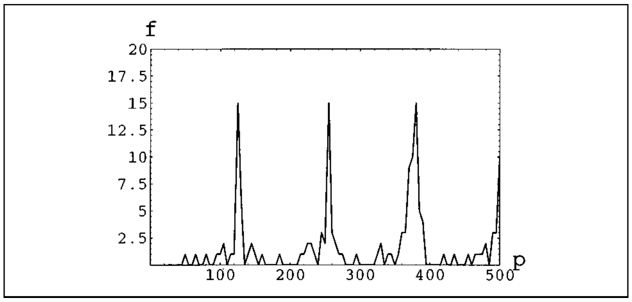

Figure 10. Frequency histogram of UPO periods p obtained with the UPO *command.*

For example, let us consider the following time series obtained from the Duffing oscillator with $f=0.39$.

```
orb=Drop[#,-1]&/@
  OrbitFlow[Duffing[0.39,1],{x,v,z},{0,1,0},{0,500,0.001}];
```

The commands UPO, UPOFrequencies (to obtain the frequencies of UPOs of different periods), and UPOHistogram (to obtain a histogram of the frequencies, as shown in Fig. 10) help us to understand the interwoven structure of UPOs within the given series.

```
upos=UPO[orb,0.01,500];
UPOFrequencies[upos]
UPOHistogram[orb,500]
     {{50,1},{62,1},{78,1},{91,1},{100,1},{101,1},{105,1},{113,1},{119,1},
     {123,1},{124,10},{125,4},{126,5},{129,1},{139,1},{141,1},{145,1},
     {149,1},{158,1},{183,1},{213,1},{218,1},{221,1},{222,1},{228,1},
     {229,1},{235,1},{244,1},{245,2},{246,1},{248,1},{252,2},{253,2},
     {254,4},{255,7},{256,1},{259,2},{263,1},{264,1},{266,1},{275,1},
     {292,1},{323,1},{328,1},{329,1},{337,1},{344,1},{351,1},{359,2},
     {360,1},{361,1},{363,1},{364,1},{366,1},{367,1},{368,1},{369,3},
     {370,3},{371,3},{372,4},{374,2},{375,1},{376,5},{377,5},{379,2},
     {380,3},{382,3},{383,1},{385,1},{386,1},{387,1},{388,1},{390,1}}
```

Finally, some of the obtained UPOs can be plotted by using the SelectUPO[timeseries,{minper,maxper}] command, which selects from the time series all the unstable orbits of periods in the range $p=minper$ to *maxper*. For example, Fig. 11 shows several UPOs with periodicities associated with the peaks of Fig. 10 (124, 252, 376).

```
UPOPlot[orb,SelectUPO[upo,{#,#}]]& /@ {124,252,376}
```

III. CONTROLLING AND SUPPRESSING CHAOS

As we have shown in Sec. II, chaotic systems are characterized by an exponential separation of nearby orbits in time. This feature of chaos has been traditionally seen as a troublesome property, especially in practical settings, because even the tiniest perturbation might modify the system's behavior in an unpredictable way and lead the system to a catastrophic situation. Chaotic behavior is therefore undesirable in many practical settings, and one is interested in controlling the system to obtain regular behavior. This can be done by taking advantage of the infinite number of UPOs coexisting with the chaotic attractor (orbit complexity). The idea of controlling chaos consists of stabilizing some of these unstable orbits, thus leading to regular and predictable behavior.

This idea was first suggested by Ott, Grebogi and Yorke.[8] They proposed a method [known as the Ott–Grebogi–Yorke (OGY) method] to stabilize UPOs containing a saddle-node point (an unstable fixed point with stable and unstable manifolds). The algorithm waits until the system comes into a small neighborhood of the saddle node. Then a small perturbation is applied to some accessible system parameter leading the orbit to the stable manifold of the saddle point, thus stabilizing the UPO. This method was experimentally applied in Ref. 11.

Since the above authors' work, much attention has focused on controlling chaos and several alternative methods

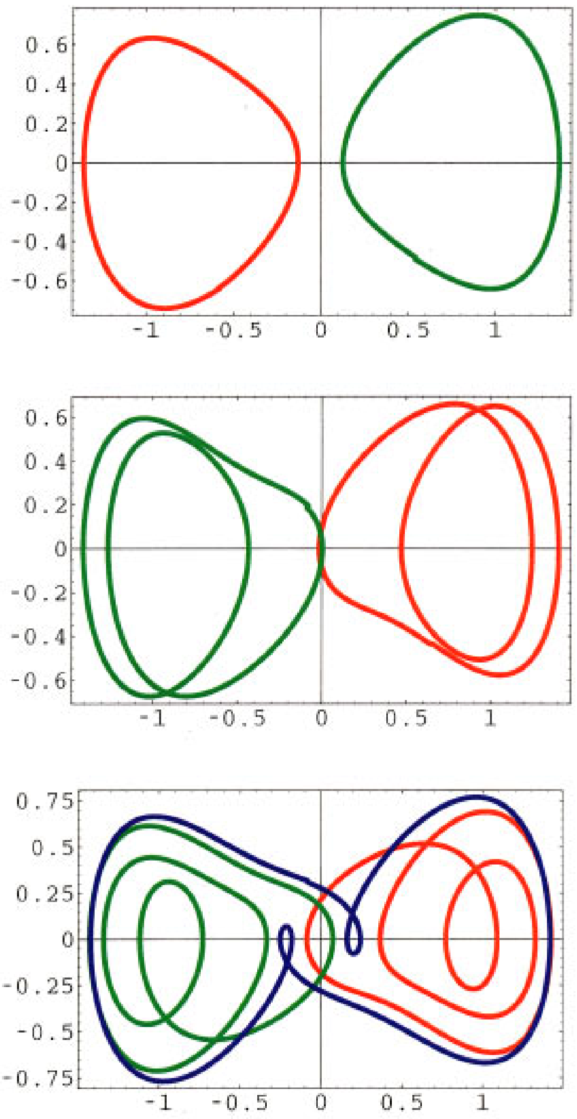

Figure 11. Period-one, -two, and -three UPOs of the Duffing oscillator.

have been proposed for a survey on controlling chaos.[12,13] The possibility of controlling chaos is changing the poor reputation of chaotic systems, since they can be seen as an unlimited reservoir of different behaviors. This flexibility may be very advantageous in many practical situations, and thus some of the chaos-control techniques that will be mentioned below have been applied to mechanical systems,[11] chemical reactions,[14] electronic circuits,[15] chaotic lasers,[16] etc.

In general, these methods can be classified into two categories: chaos-control and chaos-suppression algorithms. On the one hand, chaos-control methods, such as the OGY algorithm, have the common feature that the final controlled state is a UPO of the original system. Examples of these methods are the proportional feedback method,[14–17] the occasional proportional feedback (OPF),[14] and the small time-dependent continuous perturbations.[17]

On the other hand, those methods that work on an auxiliary system leading to a controlled state that does not really belong to the original system are referred to as chaos-suppression algorithms. Some of them are designed to follow a prescribed goal dynamics.[18–20] For instance, Hübler considers a resonant control method that modifies the original system such that the goal dynamics become a stable solution of the auxiliary system. Another alternative for chaos suppression is based on the effects of stochastic and periodic perturbations of the system.[21–24] The addition of noise[25] or the addition of constant pulses to the system variables[26] represents other ways to suppress chaotic behaviors.

With the aim of illustrating the advantages and shortcomings of both methodologies, we describe two different algorithms: the linear feedback algorithm for controlling chaos and a recently introduced suppression algorithm that works by adding constant pulses to the system variables.

A. Controlling chaos: Linear-feedback methods

Feedback control has been recognized to be useful for stabilizing unstable periodic orbits.[13,17] In fact, linear feedback has been extensively used within the framework of linear systems.[27] Now we consider the case of nonlinear chaotic systems, namely, the logistic map and the Duffing oscillator.

Let us first consider the simple case of maps. It has been proven[13] that a linear-feedback controller of the form $u_n=-\mathrm{k}v_n$ can control chaotic motion for some constant feedback k and v_n holding, $v_n \rightarrow 0$ as $\mathrm{n}\rightarrow\infty$. Under certain conditions, this linear-feedback control can lead the chaotic system to stable motion. A usual and simple choice for v_n is $v_n=x_n-p$, where p is an unstable period-one fixed point of the system. The command `FeedbackControl[map, upo, k, x0, a, b]` implements the above control algorithm, where `upo` is an arbitrary UPO of the system. First, a iterations of the map are performed without applying the control method in order to show the original dynamics. Then, the method is switched on the next b steps.

For example, consider the unstable period-one orbit of the logistic map for $r=3.9$ (as obtained in Sec. I).

```
PeriodicPoints[Logistic[3.9],x,1]
{0.,0.74359}
```

In this case, a controller of the form $u_n=-\mathrm{k}v_n=-0.95\ (x_n-0.74359)$ stabilizes the chaotic system to the desired fixed point (see Fig. 12).

```
upo={0.74359};
FeedbackControl[Logistic[3.9],upo,0.95,0.1,3000,3000]
```

In this case, the effect of linear-feedback control can easily be interpreted with the help of the bifurcation diagram of the controlled system as a function of the control parameter k. Due to the universal character of the bifurcation route for unimodal maps, the controlled map also exhibits a bifurcation route (shown in Fig. 13), with the desired period-one point $x=0.74359\ldots$

```
LogisticControl[k_]:=
  Function[x, 3.9 x (1−x)+ k(x−0.74359)];
Bifurcation[LogisticControl[k],{k,0,1,250},0.5,150]
```

This algorithm can be easily extended to deal with UPOs with arbitrary periods. In this case, the controller

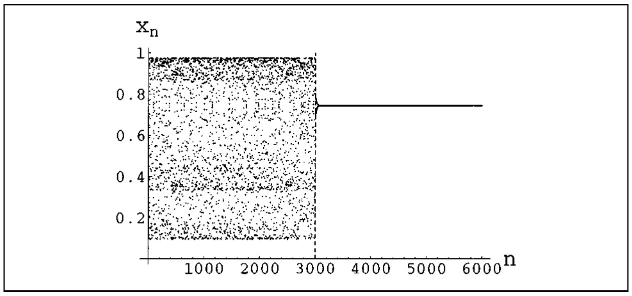

Figure 12. Period-one controlled orbit of the logistic map. The vertical dashed line shows the moment at which the chaos-control algorithm starts being applied.

takes the form $v_n = x_n - p_{\mathrm{mod}(n,m)}$, where m is the period of the UPO $\{p_1, \ldots, p_m\}$. For example, in the following we stabilize a period-3 orbit of the chaotic logistic map (Fig. 14).

```
PeriodicPoints[Logistic[3.9],x,3]
  {0.132653,0.180986,0.448718,0.578097,0.74359,
  0.951213,0.964744}
upo={0.132653,0.448718,0.964744};
FeedbackControl[Logistic[3.9],upo,0.021,0.1,3000,3000]
```

A similar idea is applied in Ref. 17 for controlling nonlinear flows. The Pyragas delayed self-controlling feedback method uses a UPO of the flow to build a feedback controller of the form $x_n = x_n - p_{\mathrm{mod}(n,m)}$, where m is the number of sampled points contained in the UPO $\{p_1, \ldots, p_m\}$. We can use here the algorithms presented in Sec. II for obtaining UPOs. For instance, consider the chaotic Duffing oscillator with $f = 0.39$ shown in Fig. 9. Suppose we want to stabilize one of the period-one UPOs obtained in Sec. II (Fig. 11). We can use the UPO and UPOSelect commands to select the desired unstable orbit, as we did before:

```
orb=OrbitFlow[Duffing[0.39,1],{x,v,z},{0,1,0},
  {0,500,0.001}];
upos=UPO[orb,0.01,500];
upo1=First[UPOSelect[upos,{124,124}]]];
```

Then, the command FeedbackFlow applies the above feedback-control algorithm to the chaotic Duffing oscillator in such a way that the system is controlled to the desired period-one motion (Fig. 15).

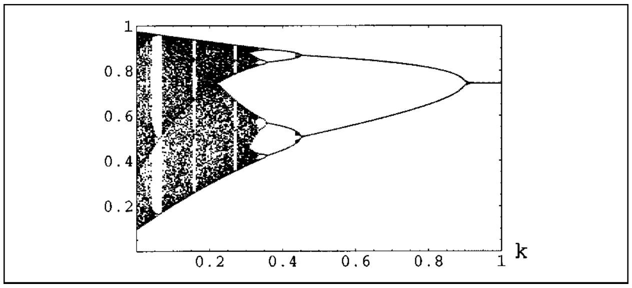

Figure 13. Bifurcation diagram of the controlled logistic map as a function of the control parameter k.

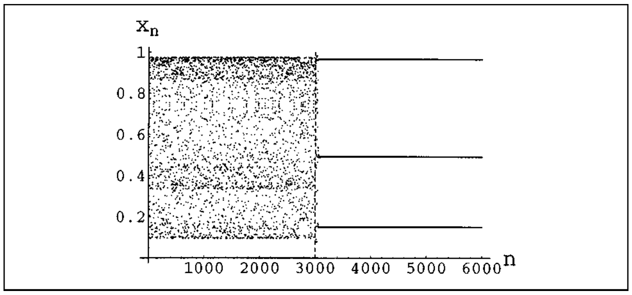

Figure 14. Period-three controlled orbit of the logistic map.

```
orb=FeedbackFlow[Duffing[0.39,1],{x,v,z},{1.,1.,1.},
  {0,150,0.05},0.13,125,v,upo1,Show→TimeSeries];
ListPlot[First /@ orb]
ListPlot[Drop[#,−1]& /@ orb]
```

In light of these examples we can conclude that feedback methods for controlling chaos can be easily implemented, can work automatically after being designed, and can be interpreted physically. These properties make these algorithms suitable for many practical applications.

B. Suppressing chaos: Adding pulses to the system variables

The feedback algorithms presented in Sec. III A allow us to stabilize the chaotic behavior of nonlinear systems by using some unstable periodic orbit embedded into the chaotic attractor. Although these methods are easy to implement, they require some knowledge about the system dynamics (especially in the case of continuous systems). Chaos-suppression algorithms allow us to stabilize the system dynamics without being concerned with the final stabilized state. The following example will help us to clarify the advantages and shortcomings between these two methodologies.

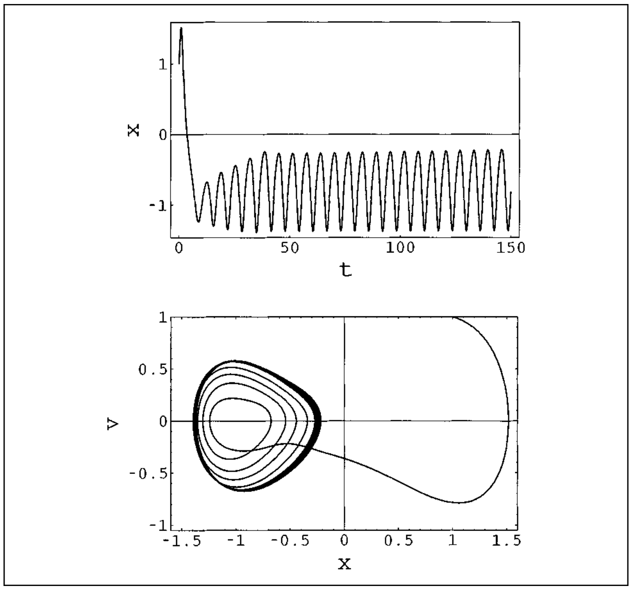

Figure 15. Controlled period-one orbit of the chaotic Duffing oscillator using the Pyragas method.

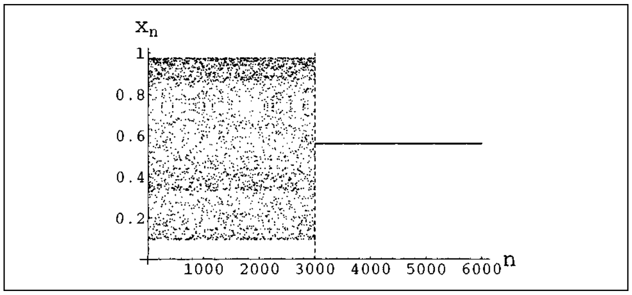

Figure 16. Stabilization of a period-one orbit with the additive chaos-suppression method.

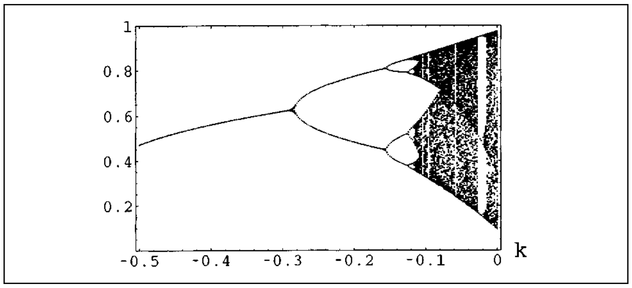

Figure 17. Bifurcation structure of the perturbed logistic map as a function of the suppression parameter k.

As an example of a chaos-suppression algorithm we consider a recently introduced method that acts on the system variables.[7,26] This method does not require any information about the system so it is, therefore, applicable even in situations where there is complete lack of information. Moreover, in many practical applications, acting on the system variables is easier than acting on the system parameters. For example, in a chemical reaction it is easy to perform changes in the system variables (by injecting or removing some components), whereas performing changes in the system parameters may be hard to do.

In the case of maps, the chaos-suppression algorithm applies a pulse of strength k to the system variables every Δn iteration steps, either in multiplicative or additive ways, in the following form:

$$x_n \to x_n(1+\delta_{n\Delta n}k) \Leftrightarrow x_n = f(r,x_{n-1})(1+\delta_{n\Delta n}k),$$

$$x_n \to x_n + \delta_{n\Delta n}k \Leftrightarrow x_n = f(r,x_{n-1}) + \delta_{n\Delta n}k,$$

where $\delta_{n\Delta n}=1$, if $\mathrm{mod}(n,\Delta n)=0$, and $\delta_{n\Delta n}=0$, otherwise. The method can be interpreted by noting that some quantity of x_n is injected into or removed from the system every Δn iterations, depending on whether k is positive or negative. The difference between the two alternatives lies in the way the pulses are introduced. In the multiplicative case, the pulse depends on the position of the system (the value of the variable) in phase space. The additive method is a simpler alternative that does not require any information about the system and, hence, is easier to apply in practical situations.

Using these methods, it is possible to stabilize chaotic systems by appropriately choosing the strength of the pulses k and the frequency of application Δn. The command SuppressMap[map, k, dn, x0, a, b] applies additive or multiplicative pulses of strength k to the system every dn iteration steps starting at the initial condition $x0$. First, a iterations are performed without applying the method to show the original system. Then, the method is switched on the next b steps. For example, the first 3000 iterations in Fig. 16 show a chaotic orbit of the logistic map. Then, the control method is switched on and a period-1 orbit is stabilized.

```
SuppressMap[Logistic[3.9],−0.4,1,0.5,3000,3000,
  Method→Additive]
```

Note that this orbit is not a true period-one orbit of the logistic map, but a periodic stable orbit of the auxiliary system

$$x_{n+1}=3.9x_n(1-x_n)+k.$$

Then, the performance of the chaos-suppression method can be qualitatively analyzed with the bifurcation structure of this auxiliary system as a function of the parameter k. Figure 17 shows the bifurcation diagram for the parameter values in the range $k=-0.5$ to 0. Note that, when the suppression method is not acting $(k=0)$, the original chaotic orbit of the system is recovered.

```
AdditiveControl[k_]:=Function[x,Logistic[39/10][x]+k];
Bifurcation[AdditiveControl[k],{k,−0.5,0,250},0.5,150]
```

We can use the commands introduced in Sec. I to obtain the values of k that stabilize the chaotic system to a periodic orbit. For instance, if we wish to stabilize the chaotic logistic map to a period-one orbit by using the additive-suppression algorithm we can proceed as follows:

```
p1=PeriodicPoints[AdditiveControl[k],x,1]
```

$$\left\{\frac{1}{78}(29-\sqrt{841+1560k}),\frac{1}{78}(29+\sqrt{841+1560k})\right\}$$

```
s1=Stability[AdditiveControl[k],k,#,x,1]& /@ p1
```

$$\left\{\{\},\{\{-\frac{841}{1560},-\frac{147}{520}\}\}\right\}$$

From the above calculations we know that the perturbed system has two period-one fixed points. The first one is never stable and the second one is stable when k is on the interval $(-(841/1560),-(147/520))\simeq(-0.539,-0.283)$. Thus, by choosing a value of k in this range $(k=-0.4)$, a period-1 orbit can be controlled (see Fig. 16). Moreover, we can choose among different values for the period-one point by substituting k in $p1$.

The pulses can also be applied in a multiplicative way. The above analytical study can also be performed in this case obtaining similar results. For example, by applying multiplicative pulses of strength $k=-0.042$, the chaotic logistic map can be switched to a periodic window where a period-6 orbit is controlled (Fig. 18).

```
SuppressMap[Logistic[3.6],−0.042,3,0.5,3000,3000,
  Method→Multiplicative]
```

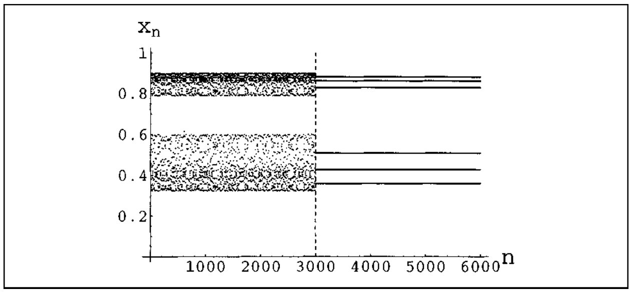

Figure 18. Suppressing chaos with small multiplicative pulses.

Using the above chaos-control method, we can switch the chaotic system not only to periodic orbits but also to any of the unstable behaviors coexisting with the chaotic system. For example, in the logistic map the transition from chaos to the period-3 window is done by an intermittent regimen. This behavior can be stabilized in the chaotic system by considering the pulses value $k=-0.04225$, as shown in Fig. 19.

```
SuppressMap[Logistic[3.6],−0.04225,3,0.5,1000,2000,
  Method→Multiplicative]
```

Therefore, when no information about the system is available, the chaos-control algorithm can be applied by trying different values for the pulses. However, when the structure of the system is known, the bifurcation structure of the controlled system will allow us to predict which pulse values are needed to control different periodic orbits. This analysis can also be performed in higher-dimensional maps.

The same algorithm can be applied to two-dimensional maps. In this case, the pulses are introduced in the system by considering the strength vector $\mathbf{k}=(k_1,k_2)$. For simplicity, we consider $k_1=k_2$, although different orbits can be stabilized by applying different pulses to each of the variables.

As an example of the application of the method, Fig. 20 shows the orbit that results from applying the chaos-control method with a strength value $k=-0.00353$ to the Hénon map. With this perturbation the system passes through an interior crisis where the strange attractor suddenly shrinks and the system is described in phase space by seven chaotic segments. In this case, chaos appears from a crisis route to chaos.

```
ControlMap2D[Henon[1.282,0.3],−0.007,1,{0.5,0.5},2000]
```

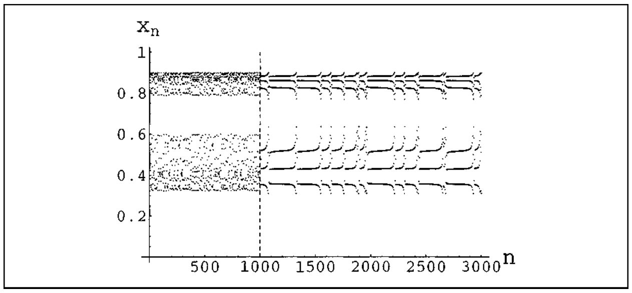

Figure 19. Switching from chaos to intermittency in the logistic map.

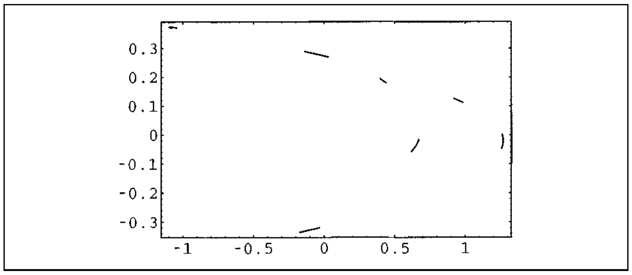

Figure 20. Suppressing chaos in the Hénon map.

Other behaviors can be similarly controlled as, for example, the quasiperiodicity route to chaos (see Ref. 28 for a more detailed explanation).

Introducing pulses into the system variables of continuous dynamical systems described by differential equations is not so intuitive as it is in the case of maps. Nevertheless, when using a numerical method to integrate the differential equations, the continuous orbit of the system is approximated by a sequence of points sampled at given time steps. Then, we can take the integration step as an arbitrary time scale for the perturbations. Thus, the chaos-suppression algorithm can be described as it is in the discrete case by perturbing the variables every Δn integration steps, in both multiplicative and additive ways.

This algorithm is implemented in the command ControlFlow[flow, x, x0, {t0,t1,dt}, k], which applies pulses to the system variables during the integration process. Our goal here is to suppress the chaotic behavior shown in Fig. 9 ($f=0.39$). For example, a period-1 orbit can be stabilized by applying pulses of strength $k=-0.025$ to x (note that v and z are auxiliary variables in this example) every $\Delta n=1$ integration steps (Fig. 21).

```
orbs=SuppressFlow[Duffing[0.39,1],{x,v,z},{0,1,0},
{0,100,0.1},{#,0,0},1,Show→TimeSeries]& /@ {0.,−0.025};

Show[GraphicsArray[{
  ListPlot[First /@ #]& /@ orbs,
  ListPlot[Drop[#,−1]& /@ #]& /@ orbs}]]
```

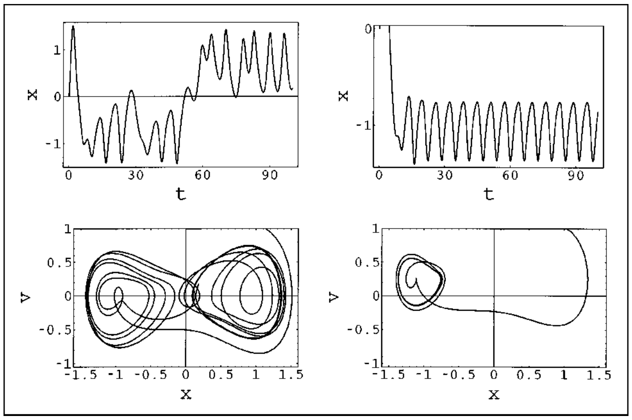

Figure 21. Time series and phase-space plot of the original chaotic (left) and the stabilized (right) orbits of the Duffing oscillator.

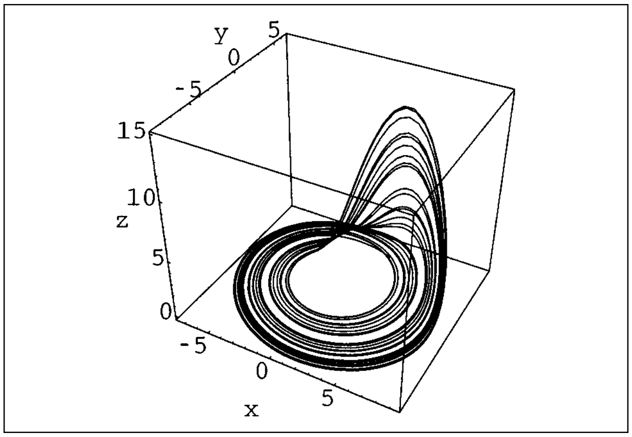

Figure 22. Chaotic attractor of the Rössler system.

In addition to having been found in the nonlinear oscillators described by nonautonomous differential equations, deterministic chaos has also been found in a great variety of three-variable autonomous continuous models in practical applications. An example of this is the Rössler model:[29]

$$\begin{cases} x' = -y - z, \\ y' = x + ay, \\ z' = b + z(x - c), \end{cases}$$

which describes a chemical process. For $a=0.2$, $b=0.2$ and $c=4.6$, the Rössler model exhibits chaos appearing through a period-doubling bifurcation route (Fig. 22).

```
Rossler={−y−z, x+0.2*y, 0.2+z (x−4.6)};
OrbitFlow[Rossler,{x,y,z},{3,3,1},{0,150,0.05},
  Show→Plot3D];
```

By applying the control method to this system, different periodic orbits from the period-doubling route to chaos can be stabilized. In Fig. 23, period-2 and period-4 orbits are stabilized by using different pulse strengths:

```
Show[GraphicsArray   [
  SuppressFlow[Rossler,{x,y,z},{1.,1.,1.},{100,150,0.05},
    {#,#,#},10,Show→Plot3D]& /@ {−0.09,−0.08} ]]
```

The above implementation of the chaos suppression method for continuous systems uses an arbitrary time scale for the perturbations. However, it would be better to apply the pulses in a natural time scale of the system. Such a natural scale can be given by a *Poincaré section*. The perturbations can then be introduced in the flow each time the system crosses the Poincaré section. This technique is common within the framework of chaos-control methods (for example, it is the key concept in the OGY method).[8] Thus, the continuous system can be controlled by simply controlling an associated Poincaré map, that is, a discrete map.[30] For example, the flow of the Rössler system is normal to the plane $x=0$. This plane can be taken as a Poincaré section of the system. Then, in order to introduce the control method into a natural time scale of the system, the pulses should be applied to variables y and z each time the system crosses the Poincaré section (given by the condition $x=0$). This section can be specified in Mathematica using the Boolean condition x0<0 && x1>0, where $x0$ and $x1$ are the x values of two consecutive sampled points, $(x0, y0, z0)$ and $(x1, y1, z1)$, that result from the integration procedure. The command SuppressPoincare implements this algorithm. Figure 24 illustrates its application to the Rössler model.

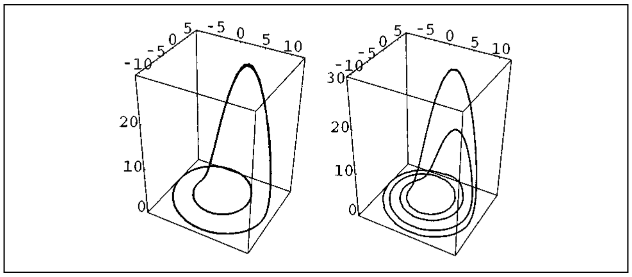

Figure 23. Suppressing chaos in the Rössler system with pulses of −0.09 and −0.08, respectively.

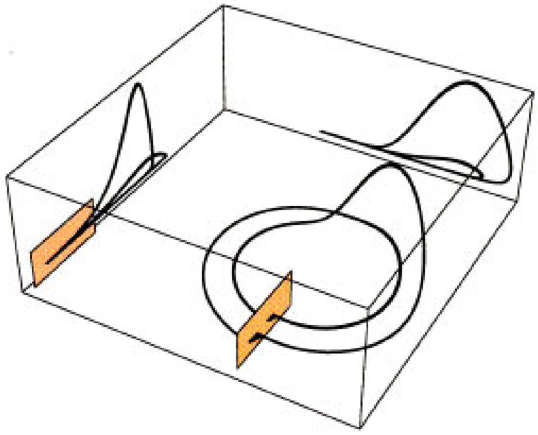

Figure 24. Suppressing chaos in the Rössler system by introducing pulses in the Poincaré section (indicated by the rectangle).

```
g=SuppressPoincare[Rossler,{x,y,z},{1,1,1},{100,150,0.05},
{0,−0.12,−0.12},x0<0     &&     x1>0,{x0,y0,z0},{x1,y1,z1},
Show→Plot3D];

poly={Thickness[0.02],Polygon[{{0,−3,−1},{0,−3,2},
{0,−10,2}, {0,−10,−1},{0,−3,−1}}]};
Shadow[Show[{g,Graphics3D[poly]},Shading→True],
  ZShadow→False, PlotRange→All]
```

ACKNOWLEDGMENTS

The authors are very grateful to Professor P. Abbott for his interest in their work and for suggesting that they write this article. They thank Caja Cantabria and the University of Cantabria for financial support of this work.

REFERENCES

1. S. Wolfram, *The Mathematica 3.0 Book* (Wolfram Media/Cambridge University Press, Cambridge, 1996); *Mathematica: A System for Doing Mathematics by Computers* (Addison–Wesley, Reading, MA, 1991).

2. R. May, Nature (London) **261**, 459 (1976).
3. H. G. Schuster, *Deterministic Chaos*, 2nd ed. (VCH, 1989), especially Chap. 3.
4. E. Ott and M. Spano, Phys. Today **48**(5), 34 (1995).
5. C. Grebogi, E. Ott, and J. A. Yorke, Phys. Rev. A **36**, 3522 (1987).
6. M. Hénon, Commun. Math. Phys. **50**, 69 (1976).
7. J. Güémez, J. M. Gutiérrez, A. Iglesias, and M. A. Matías, Phys. Lett. A **190**, 429 (1994).
8. E. Ott, C. Grebogi, and J. A. Yorke, Phys. Rev. Lett. **64**, 1196 (1990).
9. F. C. Moon, *Chaotic and Fractal Dynamics* (Wiley, New York, 1992).
10. D. P. Lathrop and E. J. Kostelich, Phys. Rev. A **40**, 4028 (1989).
11. W. L. Ditto, N. S. Rauseo, and M. L. Spano, Phys. Rev. Lett. **65**, 3211 (1990).
12. T. Shinbrot, C. Grebogi, E. Ott, and J. A. Yorke, Nature (London) **363**, 411 (1993).
13. G. Cheng and X. Dong, Int. J. Bifurcation Chaos Appl. Sci. Eng. **3**, 1363 (1993).
14. V. Petrov, V. Gaspar, J. Masere, and K. Showalter, Nature (London) **361**, 240 (1993).
15. E. R. Hunt, Phys. Rev. Lett. **67**, 1953 (1991).
16. R. Roy, T. W. Murphy, T. D. Maier, Z. Gills, and E. R. Hunt, Phys. Rev. Lett. **68**, 1259 (1992).
17. K. Pyragas, Phys. Lett. A **170**, 421 (1992).
18. A. W. Hübler, Helv. Phys. Acta **62**, 343 (1989).
19. E. A. Jackson and A. W. Hübler, Physica D **44**, 407 (1990).
20. E. A. Jackson, Phys. Rev. A **44**, 4839 (1991).
21. R. Lima and M. Pettini, Phys. Rev. A **41**, 726 (1990).
22. J. Singer, Y. Z. Wang, and H. H. Bau, Phys. Rev. Lett. **66**, 1123 (1991).
23. Y. Braiman and I. Goldhirsch, Phys. Rev. Lett. **66**, 2545 (1991).
24. R. Chacón and J. Díaz-Bejarano, Phys. Rev. Lett. **71**, 3103 (1993).
25. S. Rajasekar and M. Lakshmanan, Physica D **67**, 282 (1993).
26. M. A. Matías and J. Güémez, Phys. Rev. Lett. **72**, 1455 (1994).
27. C. K. Chui and G. Chen, *Linear Systems and Optimal Control* (Springer, New York, 1989).
28. A. Iglesias, M. A. Matías, J. Güémez, and J. M. Gutiérrez, in *Mathematics with Vision*, edited by V. Keranen and P. Mitic (Computational Mechanics, Southampton, 1995), pp. 207–214.
29. O. E. Rössler, Phys. Lett. A **57**, 397 (1976).
30. J. M. Gutiérrez, A. Iglesias, J. Güémez, and M. A. Matías, Int. J. Bifurcation Chaos Appl. Sci. Eng. **6**, 1351 (1996).